



Categories of chaos and fractal basin boundaries in forced predator–prey models

John Vandermeer^{a,1}, Lewi Stone^{b,*}, Bernd Blasius^b

^a *Department of Biology, University of Michigan, Ann Arbor, MI 48109, USA*

^b *Porter Super Center of Ecological and Environmental Studies, Tel Aviv University, Ramat Aviv 69978, Israel*

Abstract

Biological communities are affected by perturbations that frequently occur in a more-or-less periodic fashion. In this communication we use the circle map to summarize the dynamics of one such community – the periodically forced Lotka–Volterra predator–prey system. As might be expected, we show that the latter system generates a classic devil’s staircase and Arnold tongues, similar to that found from a qualitative analysis of the circle map. The circle map has other subtle features that make it useful for explaining the two qualitatively distinct forms of chaos recently noted in numerical studies of the forced Lotka–Volterra system. In the regions of overlapping tongues, coexisting attractors may be found in the Lotka–Volterra system, including at least one example of three alternative attractors, the separatrices of which are fractal and, in one specific case, Wada. The analysis is extended to a periodically forced tritrophic foodweb model that is chaotic. Interestingly, mode-locking Arnold tongue structures are observed in the model’s phase dynamics even though the foodweb equations are chaotic. © 2000 Elsevier Science Ltd. All rights reserved.

1. Introduction

Almost without exception biological communities are visited by perturbations that occur in a more-or-less periodic fashion. At one extreme of predictability are the highly regular photoperiod changes that provide cues for dramatic ecosystem transformations, or the only slightly less predictable hot and cold cycles of the northern seasons or the wet and dry periods of the tropical seasons. At the other extreme of predictability are the periodic landfall of hurricanes on tropical coastlines, or the landslides that devastate mountain vegetation. Many other examples could be cited (e.g. fires, tides, floods, pests and diseases, etc.). Ecosystems are continually perturbed in this periodic fashion. Because of their ubiquitousness, substantial ecological theory has been developed associated with the periodic nature of these all important forces (e.g. [1–7]).

In particular the phenomenon of predation has been an important focus of analysis. Since predator–prey systems are themselves inherently oscillatory, forcing them with a periodic function is similar to other situations of forced oscillators and the results obtained thus far correspond, at least qualitatively, with the behavior of physical forced oscillators. For example, in slightly different models, both Leven et al. [8] and Kot et al. [9] found that with weak forcing the predator–prey system corresponds to the general pattern deduced from the circle map, with regions of frequency locking generating a devil’s staircase. The frequency locked regions increase in size as forcing is intensified, yielding a well-known Arnold tongue structure. Sabin and Summers [10] found similar behavior when forcing the classical Lotka–Volterra system (with

* Corresponding author.

E-mail addresses: jvander@umich.edu (J. Vandermeer), lewi@lanina.tau.ac.il (L. Stone), bernd@lanina.tau.ac.il (B. Blasius).

¹ Fax: +734-747-0884.

density dependence), but did not attempt to find a devil's staircase or Arnold tongues. At a more general level, Rinaldi and his colleagues (e.g. [11–13]) have deduced a general pattern of bifurcation behavior that incorporates two distinct forms of chaos, one deriving from toroidal deformation at low levels of forcing and another deriving from period doubling bifurcations at higher levels of forcing. Furthermore, Rinaldi et al. [13] note that alternative attractors exist in the simple forced Lotka–Volterra system and speculate on the possibility of three or more alternative attractors existing at the same point in parameter space (although they had not yet found such a case in their numerical studies). Here we directly examine this possibility.

More complex behavior arises in multilevel trophic foodwebs when the unforced system is itself chaotic. One is then led to ask whether it is possible to synchronize a chaotic foodweb system with a periodic forcing function. In general, there is no unique definition of phase in continuous time chaotic systems, which makes it difficult to discuss mode-locking synchronization (e.g. 1:1, 2:1, $m:n$, etc.) with respect to a periodic forcing function. Recently however, Blasius et al. [14] proposed a three level chaotic foodweb model which exhibits uniform phase evolution. This feature means that the model cycles with a regular “rhythm,” or constant frequency, even though the cycle amplitudes are erratic (see Section 4). As we discuss below, for this class of chaos it is possible to achieve synchronization through periodic forcing.

In this communication we follow the lead of Leven et al. [8] and Kot et al. [9] in using the circle map to summarize the qualitative nature of periodically forced foodweb systems. Rinaldi et al. [13] noted that in the latter systems there are two distinct forms of chaos; indeed we find the same behavior in the circle map. We furthermore show that a simple forced Lotka–Volterra predator–prey model generates a classic devil's staircase and Arnold tongues, as expected from the qualitative analysis of the circle map. We extend the analysis to periodically forced chaotic predator–prey systems and show that similar Arnold tongues arise. Finally we demonstrate the existence of alternative attractors in regions of overlapping tongues, including at least one example of three alternative attractors. Furthermore, the separatrices of these alternative attractors are fractal and, in one specific case we show that the separatrix is Wada [15].

2. The circle map as model of forced periodic systems

Many conceptual ideas related to the synchronization of two oscillating systems are best understood from a study of the phase dynamics of each system. Synchronization is achieved when the phases of the two systems lock in a stable relationship (e.g. 1:1, or $m:n$). Here we will briefly examine the phase relationships involved in the synchronization of a typical foodweb system to a periodically varying environmental or ecological variable. We will discuss how a simple discrete “circle map” summarizes many of the generic synchronization transitions in more complex continuous time models.

A convenient technique to describe any periodic signal is by decomposing it into amplitude and phase variables [14,16]. This decomposition is especially useful for the study of periodically forced systems since the synchronization to the external force can always be determined with respect to the phase variable alone. In general, several methods to define the phase exist for periodic systems [16]. The phase θ varies in the range between $0 \leq \theta < 2\pi$ and uniquely describes the state of the periodic system. For example, it is possible to define the phase of a 2-level predator–prey system which admits a limit cycle solution, by the angle in phase space

$$\theta = \tan^{-1}[(P - P^*)/(V - V^*)]. \quad (1)$$

Here $P = \text{Predator (consumer)}$, $V = \text{Victim (prey, resource)}$, and the asterisk indicates the mean value of the variable in its limit cycle. The value of the phase θ captures the ratio of the predators to prey and their relative rates of growth, and thus provides a qualitative picture of the state of the predator–prey system.

When examining the dynamics of a periodically forced system it is useful to consider two phase variables, θ and φ , which represent the oscillations of the predator–prey system and the periodic forcing, respectively. The appropriate state space is a torus, and the circle map is obtained by constructing a Poincaré section through the torus by recording the phase θ of the predator–prey system, every time the periodic forcing φ takes on some specified value $\varphi = \varphi^*$. The structure of the circle map can be deduced by plotting successive values of θ on a graph of $\theta(t+1)$ vs. $\theta(t)$.

If both the predator–prey system and the forcing function have identical periodicities, and no coupling exists between them, once around the cycle of the forcing function equals once around the limit cycle of the predator–prey system, and we have $\theta(t+1) = \theta(t)$. If the periodicities of the two systems differ, once around the second system is not equal to once around the first system, and $\theta(t+1) = \theta(t) + 2\pi\Omega$. Here Ω is the ratio of the natural frequency of the predator–prey system to the forcing frequency. Finally, if the two systems are coupled, the second inevitably exerts some force f on the first, and we have $\theta(t+1) = \theta(t) + 2\pi\Omega - f[\theta(t)]$, where the periodic function f describes the interaction of the two oscillators, but its effect is felt only through θ since it is always calculated at $\varphi = \varphi^*$. The function f is most commonly approximated by the periodic function $f = k \sin \theta$, where k represents the strength of forcing. After normalizing the phases so that θ ranges between $0 < \theta < 1$, the standard circle map is obtained

$$\theta(t+1) = \theta(t) + \Omega - k/2\pi \sin(2\pi\theta) \pmod{1}. \quad (2)$$

The above discrete time circle map proves to be a superb model for characterizing aspects of the phase dynamics of more complicated continuous time models. The map has been studied in a variety of applications as k and Ω vary [17–19]. As coupling k is increased beyond the critical value $k = 1$, the map loses invertibility and has the potential to yield chaotic behavior [17,20]. It is important to note that in the above form of the circle map, the phase variable θ is modulo 1, and hence in terms of the dynamics of the circle map $\Omega = 0$ is equivalent to $\Omega = 1, 2, 3$, etc. Therefore, we can restrict the analysis in the discussion that follows to $0 < \Omega < 1$. It is useful to keep in mind that $\Omega \approx 1$ corresponds to a region that is approximately 1:1, with the frequency of the predator–prey system closely matching the frequency of the forcing. A smaller value of Ω say $\Omega = 0.2 = 1/5$, would indicate that the forcing frequency is five times higher than the predator–prey system.

The circle map is characterized by a well-known Arnold tongue structure (see e.g. [21]) some features of which we briefly review. First note, that there is a biologically important bifurcation that occurs in the non-chaotic region of parameter space. For small coupling $k < 1$ and frequency ratio $\Omega \approx 1$ a pair of fixed points exist on the circle map, one stable corresponding to a stable mode-locked solution, while the other solution is unstable. The stable mode-locked solution represents the Arnold tongue of 1:1 stable phaselocking, confined by the borders $\Omega = 1 \pm k/2\pi$. As the forcing frequency is increased and consequently Ω decreases, the two fixed points approach one another. Finally, at the critical point, $\Omega = 1 - k/2\pi$ (see Fig. 1) they both disappear in a saddle/node bifurcation and stable 1:1 locking is lost. Similarly, stable 1:1 locking is lost if Ω is increased beyond $\Omega = 1 + k/2\pi$. Note that by virtue of the circle map's symmetry the same Arnold tongue structure may be found at $\Omega = m \pm k/2\pi$, representing m :1 modelocking for any integer m (see Fig. 1 for $m = 0$ and $m = 1$).

It is important to note that the bifurcation at the border of these relatively large (m :1) Arnold tongues governs the behavior of the circle map at its transition to chaos. The qualitative nature of the transition to chaos, by increasing coupling strength k , depends on whether the system has gone through this bifurcation or not. To understand this, consider first the regime $1 + k/2\pi > \Omega > 1 - k/2\pi$, which contains the 1:1 Arnold tongue. In biological terms this means that the frequency difference between the oscillations of the predator–prey system and its forcing function is small relative to the coupling k of the systems. As the bifurcation diagram in Fig. 2(a) demonstrates, when k increases beyond the critical point $k = 1$, the system exhibits period doubling cascades until it approaches a chaotic state at approximately $k = 3.6$. Such behavior has been analyzed in some detail elsewhere [20].

However when the forcing frequency is increased so that $\Omega < 1 - k/2\pi$, the behavior is qualitatively different and corresponds to that usually focused on in discussions of the circle map [17,18,21]. Oscillations occur and are either phase locked or not. In the latter case the system is referred to as quasiperiodic. As k increases from $k = 0$, phase-locked regimes become more prominent and broaden out, until at $k = 1$ these regimes begin to overlap. In these regions of overlap there is a competition between the different possible oscillatory frequencies in the map's dynamics [17,18] and the quasiperiodicity route to chaos follows soon after k increases beyond $k = 1$ (see Fig. 2(b)).

From a biological perspective these results suggest that the ultimate behavior that a forced predator–prey system exhibits as forcing increases, will depend on the relative similarity of the periodicities to start with. If the forcing function has a periodicity substantially different from the free predator–prey system the

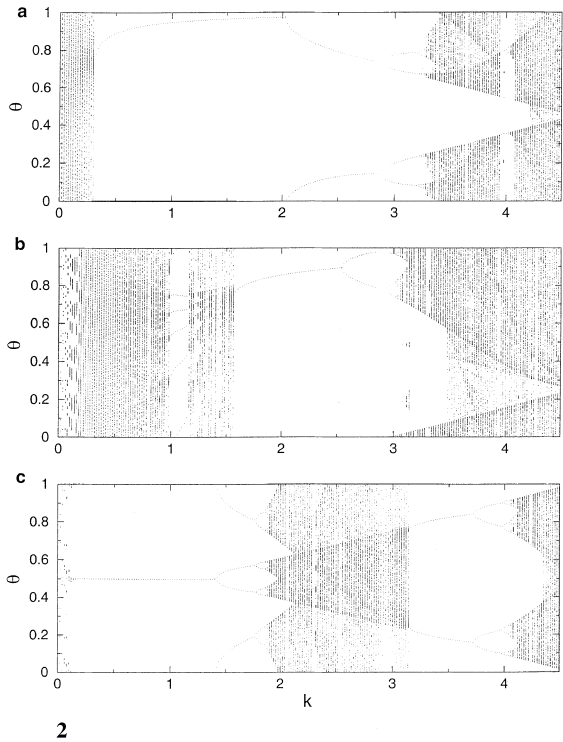
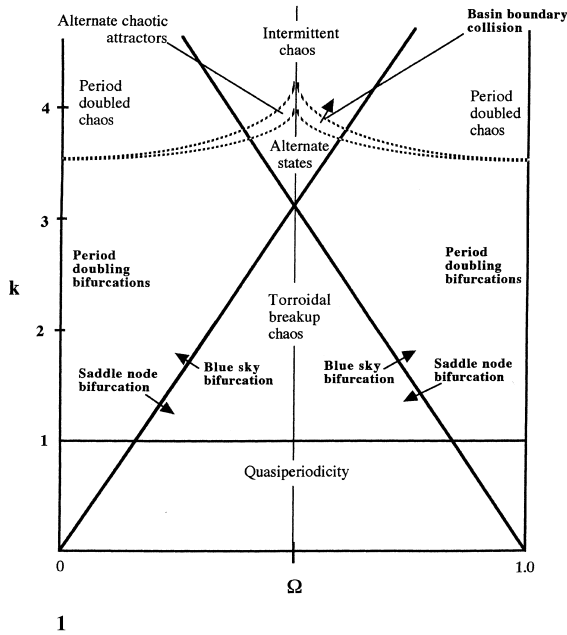


Fig. 1. Graphical summary of general bifurcation behavior as deduced from the standard circle map.

Fig. 2. Bifurcation diagrams of the circle map (2) as a function of k for different values of Ω : (a) $\Omega = 0.95$, (b) $\Omega = 0.75$ and (c) $\Omega = 0.5$, where there are two different coexisting attractors.

forced system is likely to fall into chaotic behavior much more easily than two systems that have similar natural frequencies (i.e. lying within the 1:1 tongue). This is because the critical point for the former is at the loss of invertibility ($k = 1$) while the critical point for the latter is approximately $k = 3.6$ (Fig. 1) as can be determined numerically (see Vandermeer [20] for full details).

The line $k = 2\pi(1-\Omega)$ is a bifurcation line in the sense that crossing of either parameter k or Ω results in a bifurcation of some sort. For example, if $\Omega = 0.75$, as coupling increases to $k > 1$, the system becomes chaotic through the quasiperiodic mechanism as shown in the circle map's bifurcation diagram of Fig. 2(b). But as k increases further, as it passes the value 1.57, the line $k = 2\pi(1-\Omega)$ is crossed, creating a blue sky bifurcation (see Fig. 1; [22]). At this point an unstable and stable pair of equilibria are created, while the chaotic dynamics are destroyed. Then, as coupling increases yet further, period doubling ensues until $k = 3.1$, at which point the system has period doubled to chaos. On the other hand, for larger values of Ω (Fig. 2(a), $\Omega = 0.95$), the bifurcation diagram shows that the latter quasiperiodic route to chaos may be totally bypassed since the blue sky bifurcation occurs well before Arnold tongues begin to overlap at $k = 1$.

The bifurcation behavior of the whole system is summarized in Fig. 1, where it is clear that behaviors other than those described above are also likely. With $\Omega \approx 0.5$ (i.e., the driving frequency is about double the natural frequency), and coupling of the order of 3–4, alternate basins of attraction surround two alternative attractors (see Fig. 2(c)). If k increases, both of the alternative attractors undergo a complete period doubling to a chaotic state, in which case there are alternate chaotic attractors. Further increase in k results inevitably in the basins colliding, in which case both chaotic attractors will have access to one another, leading to a situation of intermittent chaos. Yet other complications arise as k increases further (not illustrated in Fig. 1), associated with the repeated crossing of the standard circle map with the 45° line. The qualitative pattern of these extreme circumstances has been described by Zeng and Glass [23]. Suffice it to say that such extreme situations result in multiple attractors and multiple basins.

These results are consistent with numerical solutions of the forced Lotka–Volterra system by Rinaldi and his associates [11–13], in which two distinct zones of chaos were found. The region of torroidal deformation in Fig. 1, which represents the quasiperiodic route, corresponds to one form of chaos, while the chaos resulting from period doubling cascades corresponds to the other. From Fig. 1 we can also make some qualitative generalizations about what to expect from the forced system. For example, at a particular value of Ω , as the forcing coefficient, k , is increased, we expect the system to enter a regime of quasiperiodicity, perhaps arriving at a chaotic state through torroidal breakdown, but eventually returning to a relatively stable limit cycle through a saddle node bifurcation. Further increase in k should lead to a regime of period doubling, eventually resulting in chaos. If $\Omega \approx 0.5$, the zone of period doubling may not appear, but rather a regime of alternate attractors follows the chaos induced by torroidal breakdown, followed by intermittent chaos resulting from a basin boundary collision.

3. Phase-locking in periodically forced predator–prey systems

We employ the set of equations

$$\begin{aligned} \frac{dP}{dt} &= \frac{r_1VP}{b+V} - mP, \\ \frac{dV}{dt} &= [r + k \sin(\omega t)] \frac{(K-V)V}{K} - \frac{aVP}{b+V}, \end{aligned} \tag{3}$$

where P is predator, V the prey (victim), b the shape parameter of the functional response, r_1 the conversion rate of prey to predator, m the death rate of the predator, K the carrying capacity of the environment for the prey, and a is the predation rate. The periodic forcing has intensity k and angular frequency ω . In all that follows we set,

$$\frac{r_1}{m} > \frac{K+b}{K-b} \tag{4}$$

such that the unforced system is always in a limit cycle. Beyond the simple result that chaos results from forcing the oscillating predator–prey system, more qualitative patterns are evident, as described by many other authors (e.g. [1–3,5–13]). To further examine those patterns we consider the winding number [20]. Let n_i be the number of predator–prey cycles completed over a single series of i seasons as defined by the periodic seasonal forcing. We here define the winding number as

$$w = \lim_{i \rightarrow \infty} \frac{n_i}{i} \tag{5}$$

to quantify the average number of predator–prey cycles per season in the forced system.

Taking $k = 0.002$, the winding number w was computed for a range of values of ω , and the results are illustrated in Fig. 3. If we interpret ω as a measure of the “frequency of the season”, one can see that the number of predator–prey cycles per season, w , generally decreases with increasing frequency of seasonality, a natural expectation, but at various points the cycles per season are fixed over a relatively large range of seasonal frequencies. Furthermore, this pattern is fractal in that any small section of it when magnified, repeats the same qualitative pattern, as illustrated in Fig. 3. In that figure, the small box between seasonal frequencies 0.06 and 0.07 is magnified in the inset in the upper right of the figure. Clearly the step-like nature of the frequencies is obvious. This is a classical case of a “devil’s staircase,” so named because of the infinite number of steps at any magnification. Furthermore, each of the “steps” in the staircase represents a rational locking frequency and there are an infinite number of steps each positioned at a rational locking frequency. In Fig. 3 it is easy to see several of those frequencies, as indicated on the figure (e.g. one cycle per one season, one cycle per two seasons, one cycle for three seasons in the main figure, and five cycles per 13 seasons, eight cycles per 21 seasons, three cycles per eight seasons, and 10 cycles per 27 seasons in the inset of the figure). The devil’s staircase has been demonstrated in more complicated forced predator–prey

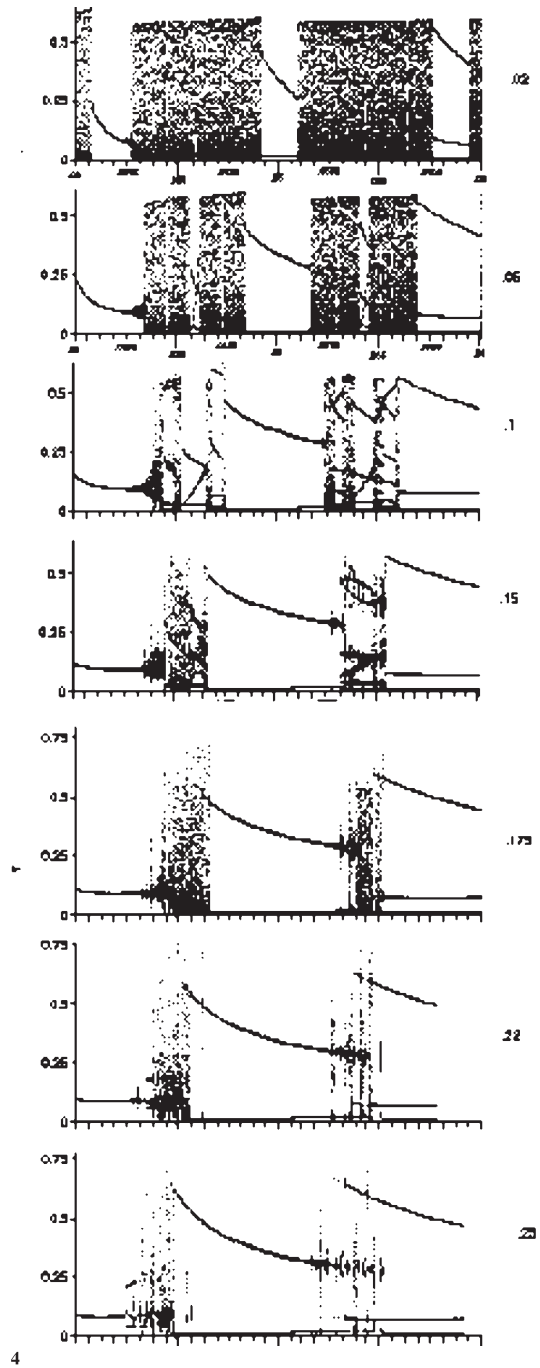
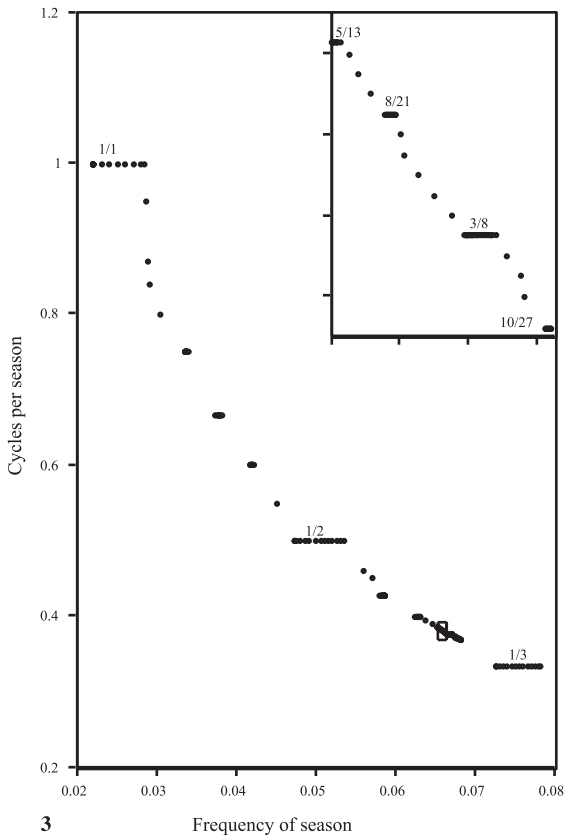


Fig. 3. Locking frequencies as a function of the seasonal frequency in system (3). Note the typical “Devil’s staircase” effect. Small box outlined between the 0.06 and 0.07 frequency is magnified in the upper inset, showing the fractal structure of the staircase. Parameter values are: $r = 0.03$, $r_1 = 0.5$, $b = 0.5$, $m = 0.1$, $K = 1$, $a = 0.05$.

Fig. 4. Points of the Poincaré section as a function of the seasonality coefficient ω repeated for different values of the strength of forcing k ($k = 0.02$ to $k = 0.25$ from top to bottom). The windows of phase locking increase as k increases. The windows are clearly overlapping in the bottom graph. Parameter values as in Fig. 3.

models [8,9], but this is the first time it has been shown for this simple system. On the other hand, its existence is not particularly surprising since we are dealing with a forced oscillator whose qualitative behavior ought to correspond to the results of the basic circle map [17,18].

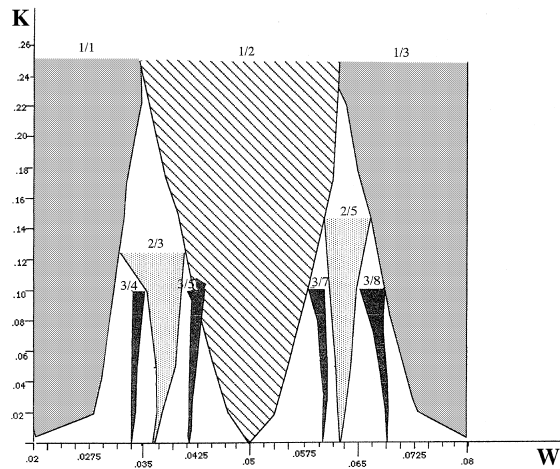


Fig. 5. Summary of the “windows” of phase locking. Abscissa is the seasonality coefficient ω and ordinate is the strength of forcing k . Regions of particular phase lockings take on the appearance of Arnold tongues (see text).

Patterns not observable from simple examination of phase space frequently become more clear when examining the Poincaré section. Define the Poincaré variables (P^* , V^*) as the values of P and V when $\sin(\omega t) = 1.0$ (that is when the seasonal cycle is at its maximum). A clear pattern can be seen if we plot the Poincaré variables as a function of the seasonal parameter, ω , as shown for V^* in Fig. 4. In Fig. 4(a), three large steps in the devil’s staircase are clearly visible, and the outlines of other locking frequencies are seen as small “windows” in the general mass of trajectories. Repeating the procedure for different values of k (i.e. increasing the strength of the seasonal forcing), we obtain the series of diagrams illustrated in Fig. 4. Note how the range of particular frequency lockings become larger, but as they become larger, take up the values of ω that previously generated other frequency lockings. Fig. 4 is centered on the $1/2$ window. Moving from the top graph to the bottom graph (in Fig. 4) the $1/2$ locking frequency becomes even larger, seemingly intersecting the $1/1$ and $1/3$ locking frequencies in the bottom graph. This general process whereby the steps of the devil’s staircase become larger as the strength of a forcing oscillator increases, leads to a widening in the Arnold tongues [8,9,17,24] as illustrated better in Fig. 5 for the present model.

Fig. 5 is a useful summary of the effects of both frequency and intensity of the forcing periodicity. With very weak seasonality, only small regions of frequency lockings will be apparent (all at rational frequencies, and incorporating all rational numbers). As the intensity of seasonality increases, there is an increase in the range of seasonal frequencies that result in particular frequency lockings; that is to say, the Arnold tongues widen. For larger forcing, the Arnold tongues intersect and there is “competition” for locking frequencies; in addition alternate attractors may emerge (as discussed below). Note that the Arnold tongues described by Kot et al. [9] are strikingly different in form compared to those presented here, although the basic structure of overlapping tongues is the same.

4. “Phase synchronization” of a periodically forced chaotic foodweb model

In recent years there has been considerable interest in extending our understanding of synchronization, which has largely been derived through the study of periodic systems, by examining the unusual synchronization properties of chaotic systems. This has become a fascinating and important area of research with many applications [14,16]. Here we show that the $n:m$ modelocking and the Arnold tongue structures just discussed, have direct applications for the study of periodically forced chaotic foodweb models.

It is now well-known that chaotic dynamics can arise in a natural way in autonomous (unforced) tri-trophic foodweb models [25,26]. However, the oscillations of these models appear to lack what we term uniform phase evolution [14]. That is, the phase component of the oscillation does not increase at a uniform rate and hence the oscillation does not have the same regular “rhythm” as expected for a periodic phase oscillator. This makes the investigation of synchronization and mode locking highly complicated.

These problems led Blasius et al. [14] to design a tritrophic foodweb model that had both uniform phase evolution and chaotic amplitudes (UPCA). The unique features of the model may be easily observed in the time series of the predator population (Fig. 6). It is characterized by a highly regular oscillation; the regularity being an outcome of the model’s uniform phase evolution. Note, however, that the peak abundance level of each cycle is erratic because of the system’s inherent chaos.

Here we use a simplified variation of the model found in [27]:

$$\begin{aligned} \dot{P} &= -c(P - p_0) + \alpha_2 PC, \\ \dot{C} &= -b(C - c_0) + \alpha_1 CV - \alpha_2 PC, \\ \dot{V} &= a[1 + k \sin(\omega t)](V - v_0) - \alpha_1 CV. \end{aligned} \tag{6}$$

The above equations represent a foodweb in which the resource or vegetation V is consumed by herbivores C , which in turn are preyed on by top predators P . The coefficients a , b , and c represent the respective net growth rates of the three species in the absence of interspecific interactions (quantified by α_i). We also assume the existence of a (stable or unstable) equilibrium point (p_0, c_0, v_0) and expand the system linearly around the steady state. The quantities p_0, c_0, v_0 , may, for example, represent the influence of alternative prey and consumers that exist in the real foodweb (see [14,27]).

The model has a periodic forcing term whose frequency ω can be modified. When ω is very close to the internal frequency of the foodweb we might expect to find 1:1 phase-locking. Indeed this is the case, and the Arnold tongue structure of the model plotted in Fig. 7 indicates that there are similar $m:n$ locking regimes as in the forced Lotka–Volterra system (Eq. (3), Fig. 5). The remarkable difference now, is that although the foodweb model is “phase synchronized” to the periodic forcing, it is nevertheless still chaotic as expressed in the erratic amplitude component of the model’s cycle.

For large values of coupling k complicated dynamics can occur. For instance the forcing can destroy the chaos and periodic windows which are phase locked appear. With higher values of the coupling the Arnold tongues typically split into different segments and overlap in complicated ways leading to the formation of multiple attractors, intermittencies and dynamics at least as complex as that found in the forced Lotka–Volterra equations.

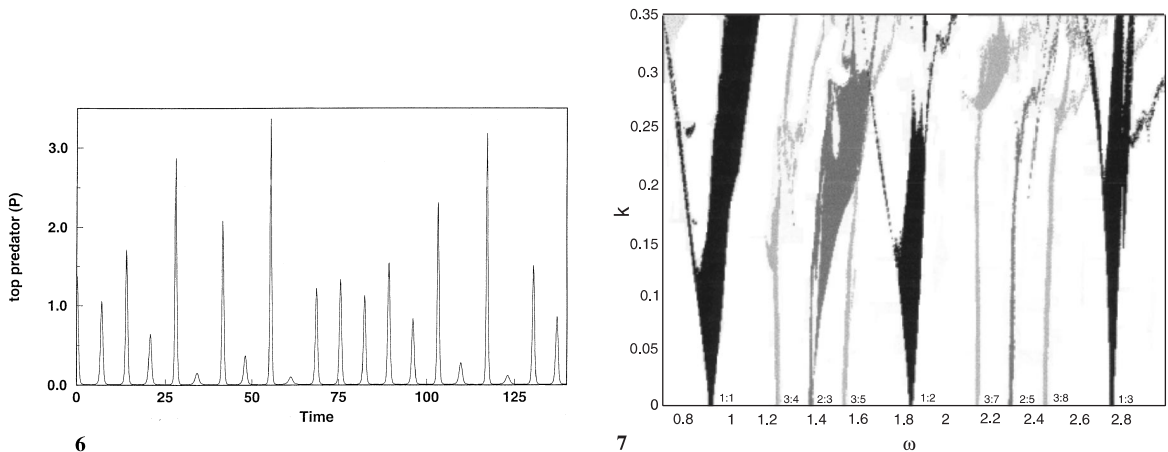


Fig. 6. Time series of the top predator P in the chaotic foodweb model (6) with UPCA behaviour (irregular amplitudes but constant period length). Parameter values are $a = 1, b = 1, c = 10, \alpha_1 = 0.6, \alpha_2 = 0.1, p_0 = 0.01, c_0 = 0, v_0 = 1.5, k = 0$.

Fig. 7. Major Arnold tongues of the forced UPCA model. Parameter values as in Fig. 6.

5. Chaotic transients, fractal basin boundaries and Wada basins

Intricate dynamics can arise when Arnold tongues overlap, including an unusual form of non-chaotic behavior. When considering parameter combinations in which there exist alternative complicated limit cycles, it so happens that the basins of these complicated cycles appear to be Wada [15]. That is, the separatrix between any two basins is also the separatrix of a third basin. The following example will clarify this observation.

We have found these complexities manifest in systems as simple in structure as the forced foodweb model Eq. (3). Similar to [12], we have analyzed Eq. (3) with seasonal forcing affecting a variety of different parameters and obtained the same qualitative results we proceed to describe for the model below, where the periodic forcing acts on the predator.

It is convenient to reformulate system (3) as an autonomous system [5]

$$\begin{aligned}
 \frac{dP}{dt} &= [r + k \sin(\Theta)] \frac{VP}{b + V} - mP, \\
 \frac{dV}{dt} &= \frac{r_1(K - V)V}{K} - \frac{aVP}{b + V}, \\
 \frac{d\Theta}{dt} &= \omega,
 \end{aligned}
 \tag{7}$$

where a new variable, Θ , has been added symbolizing the periodicity of the disturbance. This gives us a more appropriate framework for exploring the effects of the initial condition for Θ .

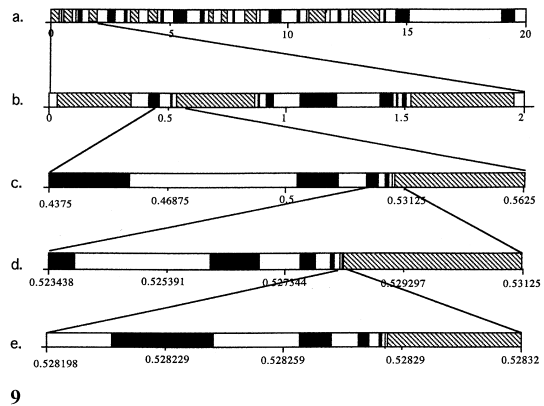
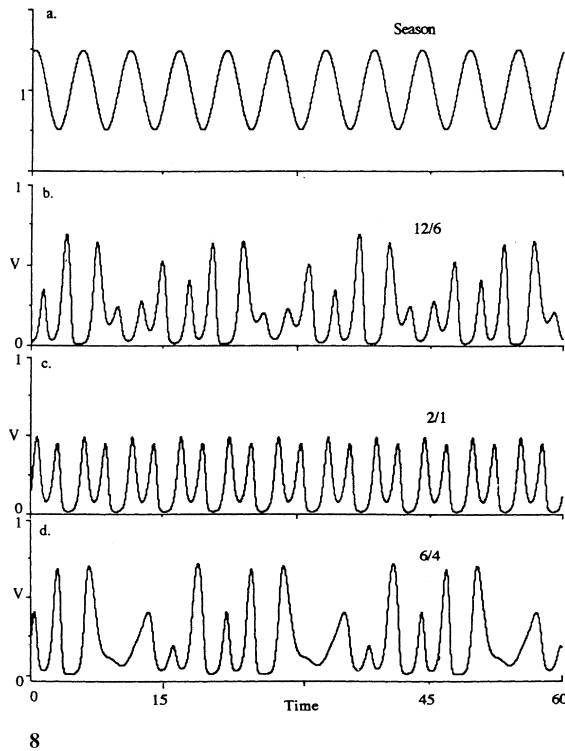


Fig. 8. The three distinct non-chaotic attractors for the system (7) with $\omega = 0.115$. Parameter values are set as follows: $r = 1$, $r_1 = 0.5$, $b = 0.5$, $m = 0.2$, $a = 0.05$, $K = 0.5$.

Fig. 9. Symbolic representation of basins of attraction for the three attractors of Fig. 8. Shaded area is 2/1 attractor, hatched area is the 12/6 attractor and white area is the 6/4 attractor. Range is the range of values of Θ at the point of initiation (V_0 and P_0 were set at 5.2 and 0.53, respectively). From top to bottom represents successive magnification of the space, illustrating its fractal nature.

Depending on the initial conditions of P , V , and Θ , one of the three attractors shown in Fig. 8 is obtained (with locking frequencies of 12/6 (Fig. 8(b)), 2/1 (Fig. 8(c)), or 6/4 (Fig. 8(d))). Thus, there are three basins of attraction, one associated with each of the three attractors. But these basins need not be continuous, nor their separatrices simple. To see this, we initiate the system at various values of Θ , asking which attractor emerges from a particular initial condition for Θ (P and V were set at 5.2 and 0.53, respectively, for all calculations). In Fig. 9 we see the results of these calculations. Not only are the basins interspersed along the Θ axis, successive magnifications of the edge of the 12/6 basin reveals the essential features of a Wada basin. That is, a point initiated near the edge of the 12/6 basin may wind up in any of the three basins, unpredictably so. Moreover, examining the size of the 2/1 sub-basins at increasing levels of magnification we see the exponential nature of their size decreases as the edge of the 12/6 basin is approached (Fig. 9).

It is difficult if not impossible to predict which basin will attract a particular trajectory unless very precise information is available about the initial conditions (see Fig. 9(a)), to say nothing of the need for precise knowledge of the parameters. But even more perplexing, with very precise information on the location of the edge of the 12/6 basin, if a point is initiated near that edge, it is in principle difficult, if not impossible, to determine which of the three basins will attract the trajectory. In this context the system is unpredictable in a very different sense than a chaotic system. Chaotic systems are quantitatively unpredictable. Here we have a system whose qualitative behavior is in principle unpredictable.

Similar results are obtained in the chaotic foodweb model (6). For instance Fig. 5 shows that near $k \approx 0.3$, $\omega \approx 1.65$ the three Arnold tongues 2:1, 2:3, 3:5 overlap. Thus when simulating system (6) with for instance $k = 0.301$, $\omega = 1.64$ we find multiple attractors which are characterized by different winding numbers.

6. Discussion

The general behavior of forced predator–prey systems, as predicted by the circle map model, is presented in Fig. 1. The two regions of chaos, one corresponding to the quasiperiodic (torroidal breakup) route, the other to the period doubling route are indicated, corresponding to the qualitative conclusions of Rinaldi and colleagues [11–13].

Periodic forcing of an elementary predator–prey model reconfirms some of the patterns reported elsewhere for similar models [2,5,8,9]. The overall qualitative pattern can be most easily conceived of as a diagram of overlapping Arnold tongues (see Fig. 5), in which locking frequencies become ever more overlapping as the strength of the periodicity increases. We have shown that these features are equally important for the phase synchronization of chaotic oscillators. This is because the dynamics of the phase variables was, in our example, largely independent of the chaotic amplitude variables.

The behavior of periodically forced systems in the areas of overlapping Arnold tongues can be perplexing given that there may sometimes be multiple coexisting attractors. For example, when $\omega = 0.120622$ in system (7) there are at least three alternative attractors. One attractor is at two cycles per year, and another is a simple multiple of that cycle giving 12 cycles every 6 yr, but the third is six cycles every 4 yr, a pattern that does not naturally emerge from the typical locking frequency scenario of the devil's staircase. Undoubtedly alternative chaotic attractors are also lurking in these zones of complicated behavior, but they are rather difficult to discern.

This basic Arnold tongue and devil's staircase structure are associated with the CHAOS 1 of Rinaldi and Muratori [11], that is, the chaos that results from torroidal deformation. At higher forcing intensity ("degree of seasonality" of Rinaldi and Muratori) the pattern is quite different, with the typical period-doubling approach to chaos. The present communication is restricted to the CHAOS 1 form. As Rinaldi and Muratori point out, the basins of attraction for the chaotic attractors in this region may be quite small and the likelihood of actually seeing a chaotic attractor might not be high. However, it is in this zone that multiple limit cycle attractors are likely to be found. It also appears that the separatrices of the basins of these alternative attractors are fractal and perhaps Wada.

When the separatrices are Wada an additional practical complication arises. For all practical purposes it is difficult if not impossible to predict which basin will attract a particular trajectory unless very precise

information is available about the starting point (see Fig. 9(a)), to say nothing of the need for precise knowledge of the parameters. But even more perplexing, with very precise information on the location of the edge of a basin (e.g. the 12/6 basin in Fig. 9), if a trajectory is initiated near that edge, it is in principle difficult if not impossible to determine which of the three basins will attract the trajectory.

The existence of alternative attractors leads to some potentially important practical results. For example along a gradient in which the strength of the seasonality is increasing (for example from south to north in North America) it could be the case that a pest insect has two cycles in the north and three in the south. Between zones of three and two cycles per year it is possible to have alternative attractors such that those exhibiting two cycles in the southern part of the northern zone might suddenly and unexpectedly switch to three cycles per year rather than the customary two (i.e. they may switch to the alternative attractor). Naturally such a qualitative result could occur with alternative chaotic attractors as well, where each of the chaotic attractors is characterized by a strict number of cycles per year even though the exact population densities are unpredictable. In either case the unpredictability is qualitatively distinct from the sort of unpredictability normally associated with chaotic attractors and could be devastating for ecosystem planning.

For example, if the attractors in Fig. 8 represent the population trajectories of a pest insect, a manager may need to know whether he or she can expect one or two cycles per season. Either the 12/6 or the 2/1 attractor represents two cycles per season (qualitatively), while the 6/4 attractor represents an average of three cycles every two seasons, effectively one or two cycles per season. Even with very precise information about the system, it will not be possible to predict how many cycles will occur. In Fig. 9(e), the complete range of starting points for θ represents 1.23 min (presuming that the forcing period is 1 yr). Thus, even if the manager knew within 1 min when the first insects emerged in the spring, predicting the qualitative nature of the oscillations would not be possible.

Acknowledgements

We thank Heather Bhasin for her help in editing and compiling the manuscript, and Minerva for the award of a fellowship to Bernd Blasius. We are grateful for support from the Adams Super Center for Brain Studies at Tel Aviv University, and an internal Tel Aviv University grant.

References

- [1] Aron JL, Schwartz IB. Seasonality and period-doubling bifurcations in an epidemic model. *J Theor Biol* 1984;110:665–79.
- [2] Inoue M, Kamifukumoto H. Scenarios leading to chaos in a forced Lotka–Volterra model. *Prog Theor Phys* 1984;71:930–7.
- [3] Kot M, Schaffer WM. Discrete-time growth-dispersal models. *Math Biosci* 1986;80:109–36.
- [4] Schaffer WM. Perceiving order in the chaos of nature. In: Boyce MS, editor. *Evolution of life histories in mammals*. New Haven: Yale University Press, 1988. pp. 313–350.
- [5] Vandermeer JH. Seasonal isochronic forcing of Lotka–Volterra equations. *Prog Theor Phys* 1996;96:13–28.
- [6] King AA, Schaffer WM, Gordon C, Treat J, Kot M. Weakly dissipative predator–prey systems. *Bull Math Biol* 1996;58:835–59.
- [7] Val J, Villa F, Lika K, Boe C. Nonlinear models of structured populations: Dynamic consequences of stage structure and discrete sampling. In: Tuljapurkar S, Caswell H, editors. *Structured-population models in marine, terrestrial, and freshwater systems*. New York: Chapman & Hall, 1997. pp. 587–613.
- [8] Leven RW, Koch BP, Markman GS. Periodic, quasiperiodic and chaotic motion in a forced predator–prey ecosystem. In: Bothe HG, Ebeling W, Kurzhanski AB, Peschel M, editors. *Dynamical systems and environmental models*. Berlin: Akademie, 1987. pp. 95–104.
- [9] Kot M, Saylor GS, Schultz TW. Complex dynamics in a model microbialsystem. *Bull Math Biol* 1992;54:619–48.
- [10] Sabin GCW, Summers D. Chaos in a periodically forced predator–prey ecosystem model. *Math Biosci* 1993;113:91–113.
- [11] Rinaldi S, Muratori S. Conditioned chaos in seasonally perturbed predator–prey models. *Ecol Model* 1993;69:79–97.
- [12] Gragnani A, Rinaldi S. A universal bifurcation diagram for seasonally perturbed predator–prey models. *Bull Math Biol* 1995;57:701–12.
- [13] Rinaldi S, Muratori S, Kuznetsov Y. Multiple attractors, catastrophes and chaos in seasonally perturbed predator–prey communities. *Bull Math Biol* 1993;55:15–35.
- [14] Blasius B, Huppert A, Stone L. Complex dynamics and phase synchronization in spatially extended ecological systems. *Nature* 1999;399:354–9.

- [15] Nusse HE, Yorke JA. Basins of Attraction. *Science* 1996;271:1376–80.
- [16] Rosenblum MG, Pikovsky AS, Kurths J. Phase synchronization of chaotic oscillators. *Phys Rev Lett* 1996;76:1804–7.
- [17] Bak P. The devil's staircase. *Phys Today*, 1986:39–45.
- [18] Bohr T, Bak P, Jensen MH. Transition to chaos by interaction of resonances in dissipative systems. II. Josephson junctions, charge-density waves, and standard maps. *Phys Rev A* 1984;30:1970–81.
- [19] Cvitanovic P, Gunaratne GH, Vinson MJ. On the mode-locking universality of critical circle maps. *Nonlinearity* 1990;3:873–85.
- [20] Vandermeer JH. The qualitative behavior of coupled predator–prey oscillations as deduced from simple circle maps. *Ecol Model* 1994;73:135–48.
- [21] Schuster HG. *Deterministic chaos*. Weinheim: Physik-Verlag; 1984.
- [22] Abraham RH, Shaw CD. *Dynamics – the geometry of behavior*. Part 4: Bifurcation behavior. Santa Cruz, CA: Aerial Press, 1988. p. 196.
- [23] Zeng W-Z, Glass L. Symbolic dynamics and skeletons of circle maps. *Physica D* 1989;40:218–34.
- [24] Jensen MH, Bak P, Bohr T. Transition to chaos by interaction of resonances in dissipative systems. I. Circle maps. *Phys Rev A* 1984;30:1960–9.
- [25] Gilpin ME. Spiral chaos in a predator–prey model. *Am Naturalist* 1979;113:306–8.
- [26] Hastings A, Powell T. Chaos in a three-species food chain. *Ecology* 1991;72:896–903.
- [27] Blasius B, Stone L. Chaos and phase synchronization in ecological systems. *Int J Bif Chaos* 2000;10 (in press).